

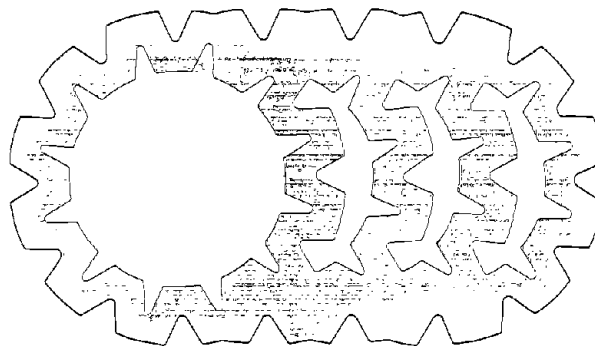


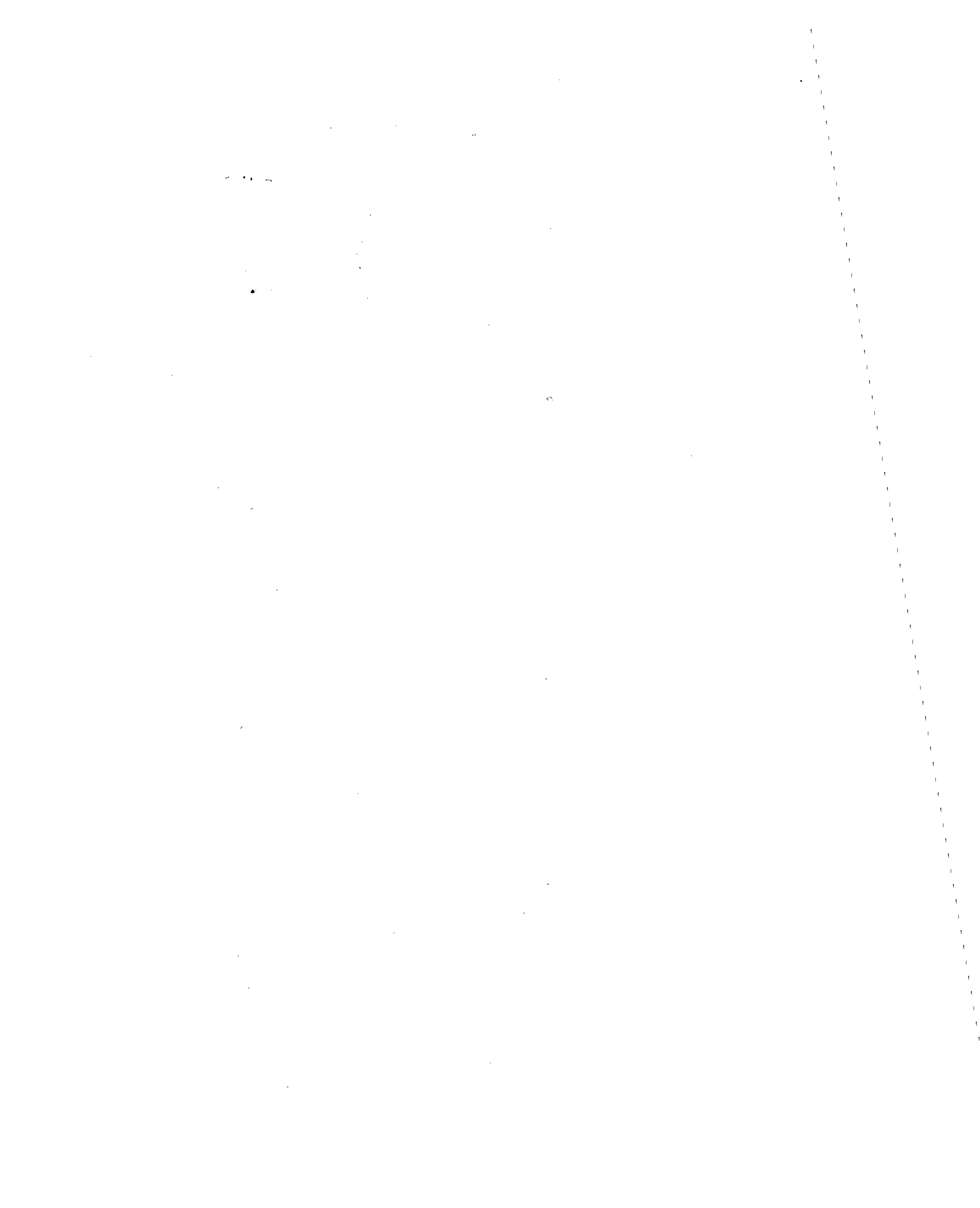
# NIOSH

TECHNICAL INFORMATION

DEVELOPMENT OF MAGNETIC

NEAR-FIELD PROBES





<b>BIBLIOGRAPHIC DATA SHEET</b>		1. Report No. NIOSH-75-127	2.	3. Recipient's Accession No.
4. Title and Subtitle Development of Magnetic Near-Field Probes			5. Report Date Jan. 1975	
7. Author(s) F. M. Greene			8. Performing Organization Rept. No.	
9. Performing Organization Name and Address Electromagnetics Division NATIONAL BUREAU OF STANDARDS Boulder, Colorado 80302			10. Project/Task/Work Unit No.	
			11. <del>Contract No.</del> Interagency Agreement NIOSH-IA-74-12	
12. Sponsoring Organization Name and Address National Institute for Occupational Safety and Health 4676 Columbia Pkwy. Cincinnati, Ohio 45226			13. Type of Report & Period Covered	
			14.	
15. Supplementary Notes				
16. Abstracts The development of two portable magnetic-field strength probes by the National Bureau of Standards (NBS) for NIOSH is described with details of the design, construction, calibrations and proper usage of the probes. Topics also include errors due to temperature variations and harmonics, electric-dipole response of a loop antenna, partial-resonance effect in a loop antenna, and the NBS conducting-plastic transmission line. The probes can be used to accurately measure magnetic near fields which exist within a few centimeters of a radiofrequency radiation source.				
17. Key Words and Document Analysis. 17a. Descriptors Magnetic field Probes Loop antennas Transmission lines				
17b. Identifiers/Open-Ended Terms Magnetic near-field probes Radiofrequency radiation Radiofrequency radiation source				
17c. COSATI Field/Group 6J				
18. Availability Statement Release Unlimited			19. Security Class (This Report) UNCLASSIFIED	21. No. of Pages 37
			20. Security Class (This Page) UNCLASSIFIED	22. Price PC A03-A01



# DEVELOPMENT OF MAGNETIC NEAR-FIELD PROBES

Frank M. Greene

Electromagnetics Division  
NATIONAL BUREAU OF STANDARDS  
Boulder, Colorado 80302

Interagency Agreement NIOSH-IA-74-12

U. S. DEPARTMENT OF HEALTH, EDUCATION, AND WELFARE  
Public Health Service  
Center for Disease Control  
National Institute for Occupational Safety and Health  
Division of Laboratories and Criteria Development  
Cincinnati, Ohio 45202  
January 1975

The contents of this report are reproduced herein as received from the National Bureau of Standards except for minor changes in the title page, the addition of a disclaimer page, a preface, a table of contents and an abstract. The opinions, findings and conclusions expressed are those of the author and not necessarily those of NIOSH. Mention of company or product names is not to be considered as an endorsement by NIOSH.

**HEW Publication No. (NIOSH) 75-127**

## PREFACE

This report describes the development of two portable magnetic-field-strength probes by the National Bureau of Standards (NBS) for the Division of Laboratories and Criteria Development, National Institute for Occupational Safety and Health. The probes were developed for the Physical Agents Branch to be used in assessing the occupational exposure from magnetic-fields. Magnetic-fields emitted by industrial radiofrequency (RF) power sources operating within the frequency range 10 MHz to 40 MHz can be accurately measured.

The purpose of this report is to explain the design, construction, calibration and proper usage of the probes. Included in this document are items of particular importance, such as detailed procedures to follow during magnetic-field-strength measurements and an analysis of the measurement errors which could occur during surveys. The reasons necessitating the use of NBS conducting-plastic transmission line to connect the probes and the readout meter are also explained.

The development of these magnetic-field-strength probes was essential to the collection of magnetic-field occupational exposure data from RF power sources. No commercially produced survey instruments were available which could be used to make meaningful magnetic-field-strength measurements between 10 MHz and 300 MHz. The Nonionizing Radiation Exposure Standard (20 CFR 1910.97, June 2, 1974) includes electromagnetic (E-M) radiation from 10 MHz to 100 GHz.

The NBS magnetic-field probes respond essentially to only the magnetic-field component of an E-M radiation field. However, commercially available E-M survey meters have virtually no magnetic-field response. Consequently, a substantial magnetic-field could be present in an E-M radiation field and the commercially manufactured meters would indicate a negligible hazard.

Due to Federal Communication Commission (FCC) regulations the vast majority of high power industrial RF radiation sources operate within the Industrial-Scientific-Medical (ISM) frequency bands specified by the FCC. The ISM bands which lie within the RF radiation range are at 13.56, 27.12 and 40.68 MHz. The NBS probes were calibrated with the greatest degree of accuracy within these ISM bands.

The NBS magnetic-field probes were calibrated for use within a few centimeters (i.e., well within the magnetic near field) of RF radiation sources. The calibration of commercial E-M survey instruments assumes that measurements will be made several wavelengths from the

E-M radiation source. This assumption is completely violated when using commercial E-M survey instruments to perform survey measurements within a few centimeters of RF radiation sources. These improper measurements are made at only a small fraction of a wavelength from the RF radiation source because at 10 MHz and 300 MHz the wavelengths are 30 meters and 1 meter, respectively. Failure to satisfy the calibration assumption could cause a sizable magnetic-field component of the RF radiation field to be totally neglected in survey measurements.

For these and other reasons which will be explained in this publication, specialized magnetic-field-strength probes are mandatory to characterize the magnetic-field component of RF radiation sources operable from approximately 10 MHz to 300 MHz.

## TABLE OF CONTENTS

	<u>Page</u>
ABSTRACT	
1. Design and Use of the NBS Magnetic-Field Probes	1
1.1 Introduction	1
1.2 The Portable H-Field Probes	1
1.3 Magnetic Field-Strength Measurements	5
1.4 Errors Due to Temperature Variations	7
1.5 Errors Due to Harmonics	7
2. The Electric-Dipole Response of a Loop Antenna	8
3. Partial-Resonance Effect in a Loop Antenna	14
4. The NBS Conducting-Plastic Transmission Line	18
4.1 Introduction	18
4.2 Conducting-Plastic Materials	19
4.3 Construction of the Conducting-Teflon Transmission Line	19
4.4 Electric Characteristics of the Conducting- Teflon Line	20
4.5 Transmission Line Attenuation	21
5. Summary and Conclusions	24



## ABSTRACT

The Nonionizing Radiation Exposure Standard (29 CFR 1910.97, June 2, 1974) includes electromagnetic (E-M) radiation from 10 MHz to 100 GHz. The relationship between the electric and magnetic fields is completely ambiguous for E-M fields within the radiofrequency (RF) region between 10 and 300 MHz. Thus, the electric and magnetic fields must be measured separately to adequately characterize the total occupational exposure from E-M fields between 10 and 300 MHz. However, no commercial RF radiation survey meters are manufactured which can be used for magnetic-field-strength measurements from 10 to 300 MHz. Thus, RF magnetic-field occupational exposure data could not be collected until appropriate instrumentation was completed.

Two portable magnetic-field-strength probes were developed for the Physical Agents Branch, DLCD, NIOSH, by NBS for use in assessing occupational exposure from industrial RF power sources. These probes consist of small, single-turn, balanced loop antennas 10-cm and 3.16-cm in diameter. Their measuring range varies with frequency but averages from approximately 0.5 to 5.0 and from 5.0 to 50 amperes per meter, respectively. The probes are specifically calibrated for use within the Federal Communication Commission Industrial-Scientific-Medical (ISM) bands at 13.56, 27.12 and 40.68 MHz but can be used at any frequency from 10 to 40 MHz. The vast majority of high power industrial RF power sources operate within one of these ISM bands.

The probes can be used to accurately measure magnetic near fields which exist within a few centimeters of an RF radiation source. Precision magnetic near field measurements are possible because of proper antenna and probe design, a thorough knowledge of measurement errors, and a detailed outline of procedures to virtually eliminate measurement errors.

V



## 1. Design and Use of the NBS Magnetic-Field Probes

1.1 Introduction. This report covers the development and construction of two portable magnetic-field-strength probes by the Electromagnetics Division of the National Bureau of Standards for the National Institute for Occupational Safety and Health [NIOSH]. These probes are intended for use in measuring hazard-level magnetic near fields in the frequency range from approximately 10 to 40 MHz. They will be used by NIOSH in their EM radiation-exposure program for determining the biological effects of hazard-level, non-ionizing EM fields on human beings.

These probes consist of small, single-turn, balanced loop antennas, 10-cm and 3.16-cm in diameter. Their measuring range varies with frequency but averages from roughly 0.5 to 5.0 and from 5.0 to 50 amperes per meter, respectively, over the above frequency range. Each loop has a type 1N4148 silicon-junction, semiconductor diode connected internally across its gap to rectify the induced r-f voltage. The d-c output of each probe is in the range from roughly 1 to 10 volts for the above range of field strengths. This d-c is transmitted over a special non-metallic, high-resistance, transmission line to a remote, high-resistance, electrometer voltmeter, located up to 30 feet away. This special conducting-plastic line was also developed at NBS.

The response of the loop probes as a function of their operating frequency and physical size will be treated in this report. In addition, measurement errors will be analyzed resulting from: (a) the electric-dipole response of the loops to the electric field present; (b) partial resonance within the loops due to their distributed capacitance; and (c) harmonic frequencies present in the fields being measured. The characteristics of the high-resistance, conducting-plastic transmission line will also be discussed in detail.

The loop probes are swivel mounted at the end of a 36-inch-long tubular fiber-glass handle, and can be either hand held or tripod mounted while making field-strength measurements. The angle between the principal axes of the loop and handle can be set for either zero degrees or 54.74 degrees to facilitate making certain types of measurements to be described in the report.

1.2 The Portable H-Field Probes. A schematic diagram of the portable loop probe is shown in figure 1. A balanced R-C, r-f filter, consisting of R-1, R-2, C-1, and C-2, is built into the handle of the probe to prevent any r-f voltage picked up on the resistance line from being rectified by the

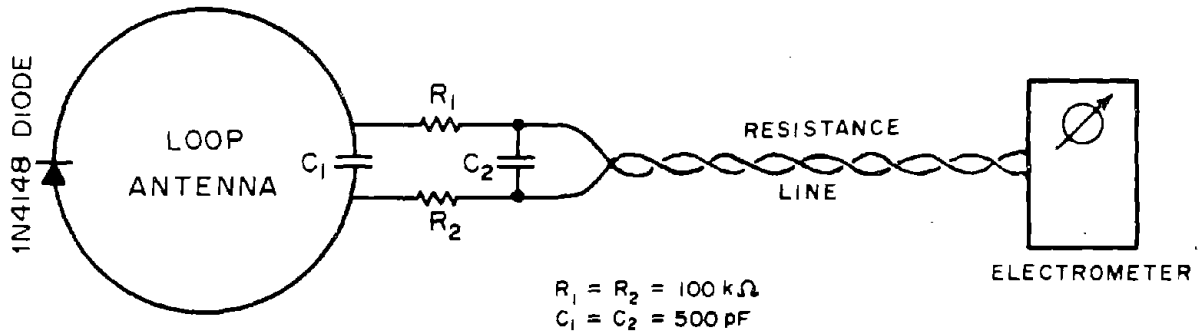


Figure 1. Schematic Diagram of the Portable Loop Probe.

1N4148 diode and causing an error in indication. The capacitor, C-1, is built into the base of the loop and serves as an r-f bypass capacitor to complete the loop r-f circuit without short-circuiting the rectified d-c output.

The equivalent circuit of the small, balanced loop antenna is shown in figure 2.  $L_a$  is the internal, low-frequency inductance

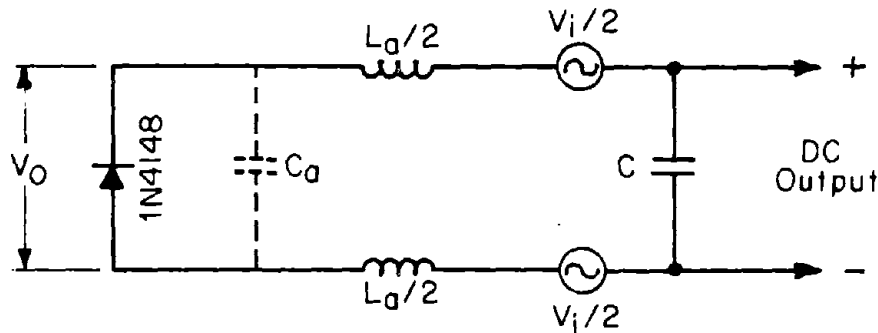


Figure 2. Equivalent Circuit of the Balanced Loop Probe.

of the loop.  $C_a$  represents the combined distributed capacitance of the loop and the gap and diode capacitances, and is what determines the partial resonance effect to be discussed later. The radiation and loss resistances are negligible for small loops in this frequency range and are being ignored in this treatment.  $V_i$  is the r-f voltage induced in the loop by the magnetic field,  $H$ .  $V_o$  is the output r-f voltage appearing across the gap and diode at the center of the loop. At low frequencies where  $C_a$  can be neglected,  $V_o \cong V_i$ .

The induced voltage,  $V_i$ , can be determined from one of Maxwell's equations relating  $E$  and  $H$  at any point. For the sinusoidally time-varying, steady-state case, this is<sup>1</sup>

$$\nabla \times \vec{E} = -j\omega\mu\vec{H}. \quad (1)$$

If both sides of equation (1) are integrated over the circular area of the loop,  $A = \pi r^2$ , and Stokes' theorem is applied, we obtain

$$\oint_0^{2\pi} \vec{E} \cdot d\vec{\ell} = -j\omega\mu HA. \quad (2)$$

$\ell$  is the circumference of the loop,  $\ell = 2\pi r$ , meters. From the Maxwell-Faraday law, the left-hand side of equation (2) is the induced voltage,  $V_i$ , in the loop. So that

$$\oint_0^{2\pi} \vec{E} \cdot d\vec{\ell} = V_i = -j\omega\mu HA, \text{ volts}, \quad (3)$$

where  $\omega = 2\pi f$ ,  $\mu = 4\pi 10^{-7}$ , and  $H$  is the normal component of the magnetic-field strength in amperes per meter, assumed constant over the area of the loop. It should be noted from equation (3) that the induced voltage,  $V_i$ , lags the magnetic field,  $H$ , by 90 degrees. This will be made use of later in evaluating errors due to the electric-dipole response of the loop.

From equation (3), the magnitude of the induced voltage can be written

$$|V_i| = 0.2\pi^3 f_{\text{MHz}} d^2 H, \text{ volts}, \quad (4)$$

where  $f_{\text{MHz}}$  is the operating frequency in megahertz;  $d$  is the mean diameter of the loop in meters. As can be seen, the response of the loop (at low-frequencies) is proportional to frequency, which somewhat complicates its calibration and use. The response is also proportional to the area of the loop,  $A = \pi d^2/4$ , in square meters. The relative responses of the 10-cm- and the 3.16-cm-diameter loop antennas are shown vs. frequency in figure 3.

<sup>1</sup>Ramo, S., Whinnery, J.R., and Van Duzer, T., *Fields and Waves in Communication Electronics*, pp. 228-242 (John Wiley & Sons, Inc., New York, N.Y., 1965).

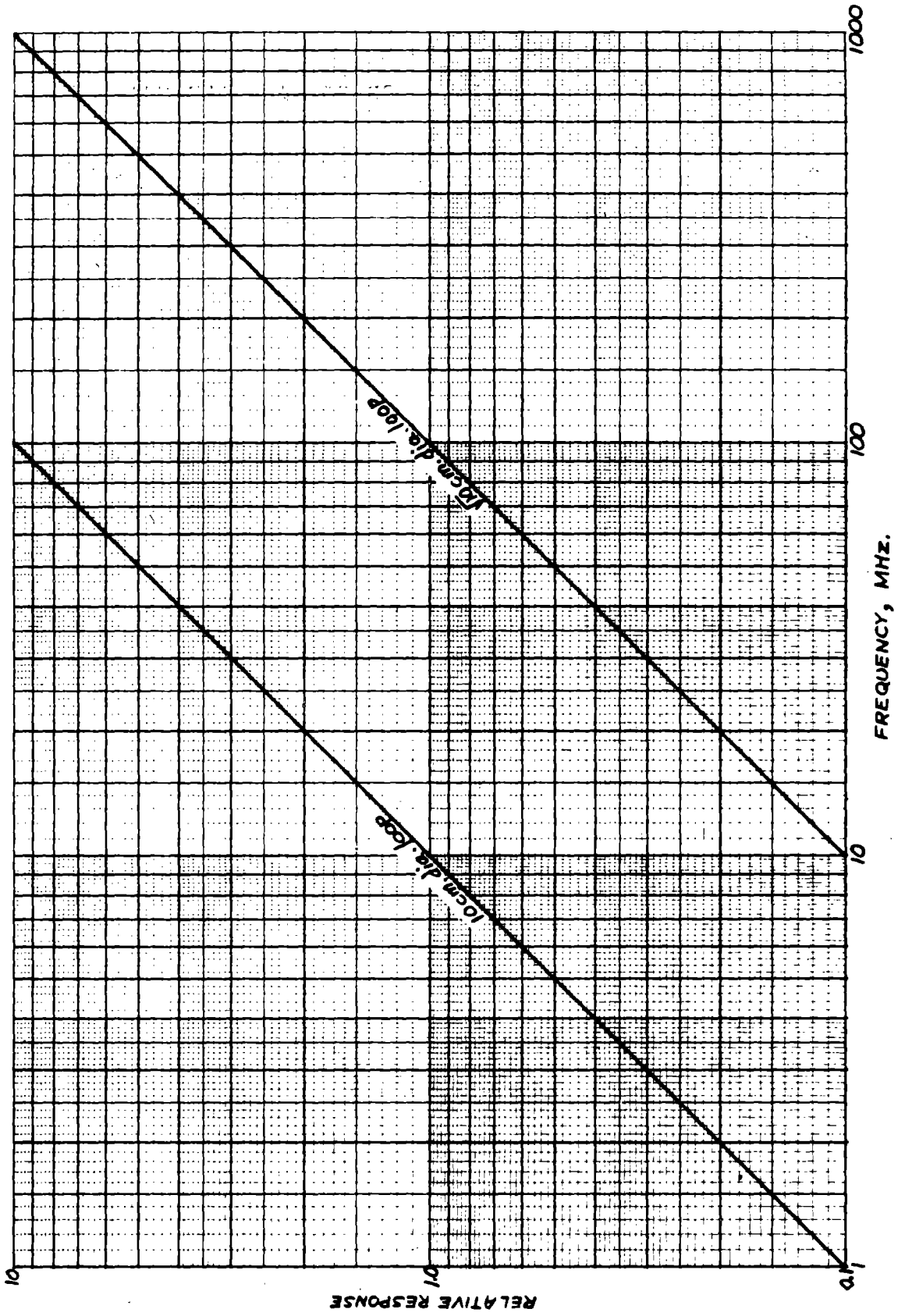


Figure 3. Relative Responses of the 10-cm and the 3.16-cm-diameter Loop Antennas.

1.3 Magnetic Field-Strength Measurements. These probes measure the component of H normal (perpendicular) to the plane of the loop (i.e., parallel to the loop axis). The units of H are amperes per meter, A/m. The detector time constant is such that the probes measure essentially the instantaneous peak value of a steady-state cw field over the measuring range involved here. This has been multiplied by 0.707 to convert the indication to rms (root-mean-square). Calibration curves are also included for the case of pulsed fields having a duty cycle of 0.05 or greater. However, the difference between the cw and the pulse calibration is small. The probes indicate the rms value of the magnetic field during the pulse, i.e., 0.707 times the instantaneous peak value of the pulse (using the calibration curve applying to the appropriate duty cycle).

The calibration curves supplied are valid for use at the frequency indicated on each curve (the probe response is proportional to frequency). When the probes are used at a frequency other than that indicated on a curve, the value of H obtained from the calibration curve must be multiplied by the factor  $(f_1/f_2)$ , where  $f_1$  is the frequency indicated on the curve being used, and  $f_2$  is the other frequency in megahertz. The measuring range for the 10 cm diameter probe at a frequency of 13.56 MHz is from approximately 1 to 10 amperes per meter for a range of d-c output from 1 to 10 volts (open circuit). This corresponds to a range of free-space electric field strength from roughly 400 to 4000 volts per meter. The approximate measuring ranges for the two probes at the three frequencies, 13.56, 27.12, and 40.68 MHz, are given in the following table:

Table I

Approximate Measuring Range of the Portable H-Field Probes

(for  $V_{dc}$  in the range 1 to 10 volts)

<u>10-cm-Diameter Loop</u>		
<u>Frequency</u>	<u>H-Field Range</u>	<u>E-Field Range*</u>
13.56 MHz	1.0 to 10 A/m	400 to 4000 V/m
27.12 MHz	0.5 to 5 A/m	200 to 2000 V/m
40.68 MHz	0.3 to 3 A/m	130 to 1300 V/m
<u>3.16-cm-Diameter Loop</u>		
<u>Frequency</u>	<u>H-Field Range</u>	<u>E-Field Range*</u>
13.56 MHz	10 to 100 A/m	4000 to 40,000 V/m
27.12 MHz	5 to 50 A/m	2000 to 20,000 V/m
40.68 MHz	3 to 30 A/m	1300 to 13,000 V/m

\*Based on the far-field case for  $E = 120\pi H$

When measuring magnetic-field strength with a loop probe, the latter is placed with its center at the point where the field is to be evaluated. If the magnitude of the field is to be determined, the loop is slowly rotated for a maximum reading on the electrometer in the 10 volt position. The value of field strength is then determined from the appropriate calibration curve. The direction of the H-field vector is the same as that of the axis of the loop when in the maximum-field position. If the vertical or horizontal component of the field is to be measured, the loop axis is simply rotated to the vertical or horizontal position and the field evaluated from the corresponding electrometer reading. The relationship between the magnitude of H and its vertical,  $H_v$ , and horizontal,  $H_h$ , components is

$$H = \sqrt{H_v^2 + H_h^2}. \quad (5)$$

This assumes that when measuring the horizontal component of the field, the loop axis is slowly rotated in the horizontal plane until the maximum-field reading is obtained on the electrometer.

It is also possible to determine the magnitude of the magnetic field, H, from any three orthogonal components at any point in space. The loop should be positioned at the 54.74-degree setting previously specified in Section 1.1. Any three probe readings are taken 120 degrees apart as the handle is slowly rotated. The magnitude of the magnetic field can then be determined from these three components,  $H_x$ ,  $H_y$ , and  $H_z$ , using the relationship

$$H = \sqrt{H_x^2 + H_y^2 + H_z^2}. \quad (6)$$

It is usually possible to make one of the components zero in equation (6) by proper pre-orientation of the probe.

When measuring H with the portable probes it will be found advantageous to set the Range Switch on the electrometer to "10<sup>-8</sup> AMPERES" (Multiplier Switch on "10"). This loads the electrometer input with 10<sup>8</sup> ohms and shortens the response time. When the desired position or reading of the probe is obtained, the Range Switch setting should be changed to "10<sup>-10</sup> AMPERES" (10<sup>10</sup> ohm input load) before the final reading is taken. With the Multiplier Switch set on "10" as above, the electrometer indicates 10 volts full scale as required for these measurements. If the Range Switch were set to the "VOLTS" position instead, the electrometer input would be loaded with 10<sup>14</sup> ohms, which would make the response time excessively long (see the instruction manual supplied by the manufacturer).

1.4 Errors Due to Temperature Variations. The probes were calibrated at NBS at room temperature (approximately 23°C). The measurement error due to temperature variations may be as much as 1 percent per °C departure from 23°C.

1.5 Errors Due to Harmonics. If harmonics are present in the field being measured, they can contribute to the measurement error. This is particularly true of a loop probe, since its principal response is proportional to frequency, as previously shown in Section 1.2. In addition, both the electric-dipole response of the loop, and the partial-resonance effect, to be discussed in Section 2 and Section 3 respectively, also increase with frequency, which can further accentuate the harmonic error. The harmonics of many transmitters are at least 30 decibels below the fundamental-frequency output of the transmitter. If the harmonics are stronger than this, it is possible to use filters in the transmitter output to further attenuate them, although many industrial transmitters probably do not.

If the levels of the harmonic fields are known, the resulting contribution to the worst-case measurement error, due to the above three factors, can be estimated by reference to figures 3, 6, and 9. Since the phase relationship between these three factors is, in general, not known, the worst that can happen is for them to add linearly to the principal response of the loop probe at the fundamental frequency.

## 2. The Electric-Dipole Response of a Loop Antenna

This section will treat the electric-dipole response of a loop antenna when measuring H. As is well known, this response will contribute to the H-field measurement error. It can be minimized in any of three ways: (a) by the use of a doubly loaded loop;<sup>2</sup> (b) by making the linear dimensions of the loop small compared to the wavelength, if a singly loaded loop is used; (c) by following a procedure, when measuring H, that will average out the electric-dipole response, as will be discussed later.

The equivalent lumped circuit of the electrically small, singly loaded loop antenna showing the electric-dipole and magnetic-dipole responses is given in figure 4. Since the loop is assumed to be small, the radiation resistance has been ignored.

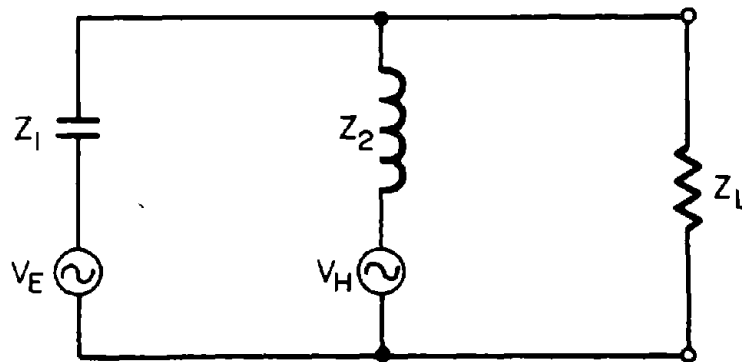


Figure 4. The Equivalent Lumped Circuit of the Electrically Small, Singly Loaded Loop Antenna Showing the Electric-Dipole and Magnetic-Dipole Responses.

$V_E$  is the induced voltage in the loop due to the electric-dipole response to the component of the electric field,  $E$ , in the plane of the loop.  $V_E = L_{eff} \cdot E$ , where  $L_{eff}$  is the electrical effective length.  $V_E$  is in time phase with  $E$ .

---

<sup>2</sup>Whiteside, H., and King, R.W.P., The Loop Antenna as a Probe, IEEE Trans. on Antennas and Propagation, Vol. AP-12; No. 3, May 1964.

$V_H$  is the induced voltage due to the magnetic-dipole response to the component of  $H$  normal to the plane of the loop.  
 $V_H = -j\omega\mu H \cdot A$ .  $V_H$  is in time-phase quadrature with  $H$ .

$Z_1 = -j/\omega C$ , where  $C$  is the low-frequency self-capacitance of the loop.

$Z_2 = j\omega L$ , where  $L$  is the low-frequency self-inductance of the loop.

$Z_L$  is the load impedance connected to the loop terminals, i.e., the diode load impedance, the gap capacitance, etc.

The total voltage,  $V_i$ , induced in the loop is the complex sum of  $V_H$  and  $V_E$ , i.e.,

$$V_i = V_H + V_E = V_H \left( 1 + \frac{V_E}{V_H} \right). \quad (7)$$

The error in measuring  $H$ , caused by the electric-dipole response, can therefore be determined from the ratio of the voltages produced across the load by  $V_E$  and  $V_H$ . Call these voltages  $V_{EL}$  and  $V_{HL}$  respectively. The error ratio, which is in general complex, is then given by

$$\frac{V_{EL}}{V_{HL}} = \frac{Z_2}{Z_1} \left( \frac{V_E}{V_H} \right) = -\omega^2 LC \left( \frac{V_E}{V_H} \right). \quad (8)$$

This ratio is independent of the load impedance,  $Z_L$ , as can be seen from equation (8). The induced-voltage ratio,  $V_E/V_H$ , is given by

$$\frac{V_E}{V_H} = \frac{j3}{4\omega\mu w} \left( \frac{E}{H} \right) \quad (9)$$

where the electrical effective length,  $L_{eff}$ , has been assumed to be equal to three-quarters of the length of one side,  $w$ , for a square loop.<sup>3</sup> Before equation (9) can be evaluated, both the magnitude and phase of the complex wave-impedance,  $E/H$ , must be known.

<sup>3</sup>Whiteside, H., and King, R.W.P., loc. cit.

For the case of a uniform plane wave, where  $E = 120\pi H$ , equation (9) becomes

$$\frac{V_E}{V_H} = j \frac{3}{4\beta w} \quad (10)$$

where  $\beta = 2\pi/\lambda$ , and  $\lambda =$  free-space wavelength, meters. When equation (10) is substituted in equation (8) along with Whiteside's expressions for  $L$  and  $C$ , his formula for the error ratio of a small, singly loaded square loop is obtained

$$\frac{V_{EL}}{V_{HL}} = -j 3\pi \left( \frac{w}{\lambda} \right) \left( \frac{\Omega - 4.32}{\Omega - 3.17} \right), \quad (11)$$

where  $\Omega = 2 \log_e(4w/a)$ , and  $a$  is the radius of the conductor forming the loop.

Since the bracketed term involving  $\Omega$  at the extreme right in equation (11) is approximately unity, if  $\Omega$  is large, the error ratio for a square loop can be approximated by

$$\frac{V_{EL}}{V_{HL}} \approx -j 3\pi \left( \frac{w}{\lambda} \right). \quad (12)$$

For a circular loop of diameter,  $d$ , the error ratio is<sup>4</sup>

$$\frac{V_{EL}}{V_{HL}} \approx -j 2\pi \left( \frac{d}{\lambda} \right), \quad (13)$$

where  $\lambda$  is the wavelength in meters. As can be seen, the error ratio is directly proportional to the electrical size of the loop,  $w/\lambda$  or  $d/\lambda$ . It can be seen from equations (12) and (13) that the error ratio for a circular loop is approximately 3.5 dB less than for a square loop, when  $d = w$ .

For the plane-wave case in which  $E$  and  $H$  are in time phase, the error ratio given by equation (13) is imaginary, as shown. In the near-field case in which  $E$  and  $H$  may approach a time-phase-quadrature relationship (in the limit as the source is approached), equation (13) becomes real in the limit, and also must be corrected for the new ratio  $E/H$  existing in the near zone. In the former plane-wave case, an error ratio of 0.1 will result in an error due to  $E$ -field pickup of only

<sup>4</sup>Whiteside, H., and King, R.W.P., loc. cit.

0.5 percent. In the near-zone case the resulting error may be as high as 10 percent or more in the limit for the same error ratio.

If the magnitude and phase angle of the wave impedance are not known, the following experimental technique can be used to minimize the error due to E-field pickup. For this test the loop should be positioned at the zero-degree setting previously specified in Section 1.1. While making an H-field measurement, the loop is slowly rotated in its own plane, about its axis. If no E-field pickup is present, the output indication of the loop should not change. If a change is noted, the correct value of H can be determined by taking the average of the high and the low readings as the loop is slowly rotated through 360 degrees.

Equation (13) can be used to estimate the worst-case error in the H-field measurements and is shown plotted vs.  $d/\lambda$  in figure 5. For a value of  $d/\lambda = 0.1$ , for example, this error may be as high as 60 percent. This error is also shown plotted vs. frequency for the 10-cm and 3.16-cm-diameter loops in figure 6.

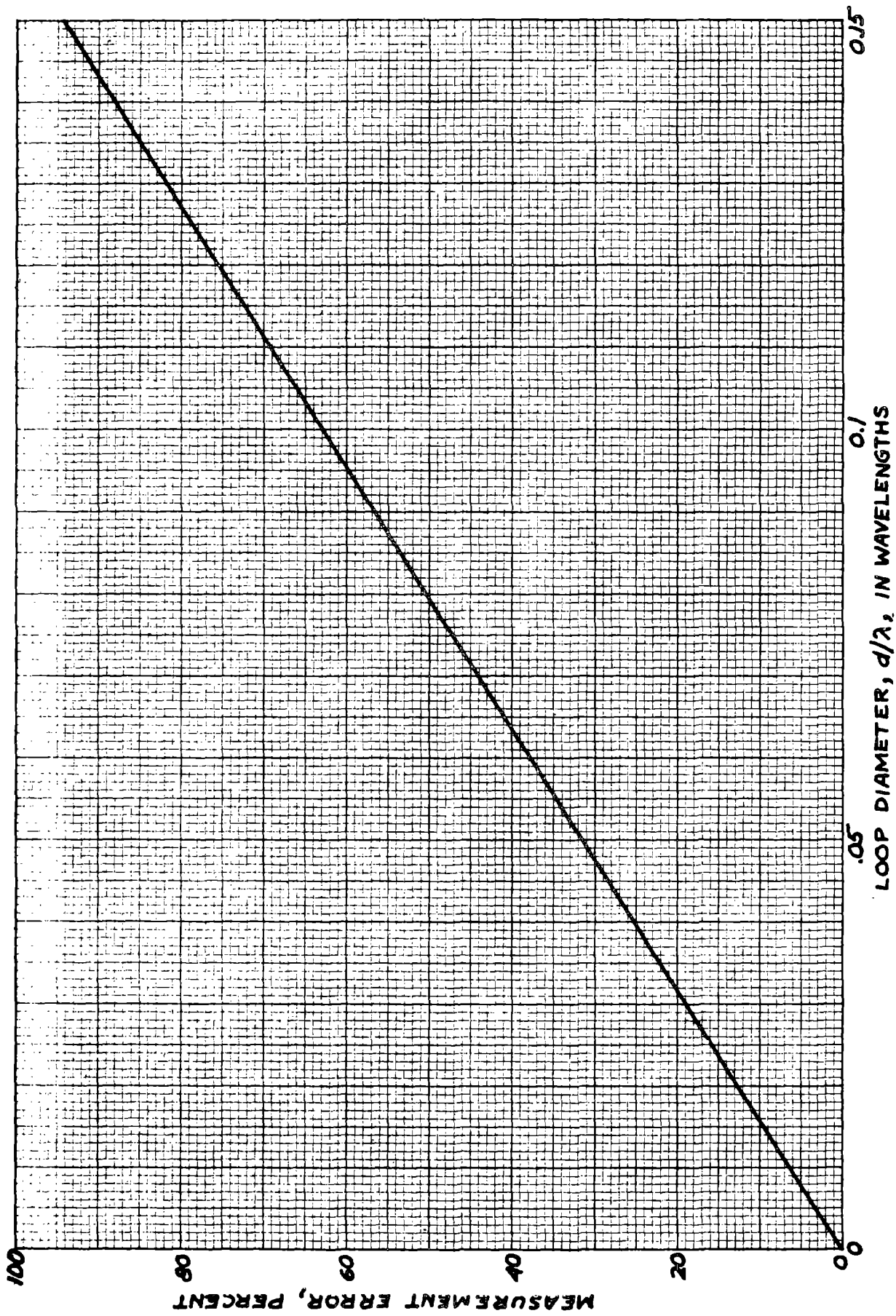


Figure 5. Worst-Case Measurement Error of a Circular-Loop Antenna due to its Electric-Dipole Response.

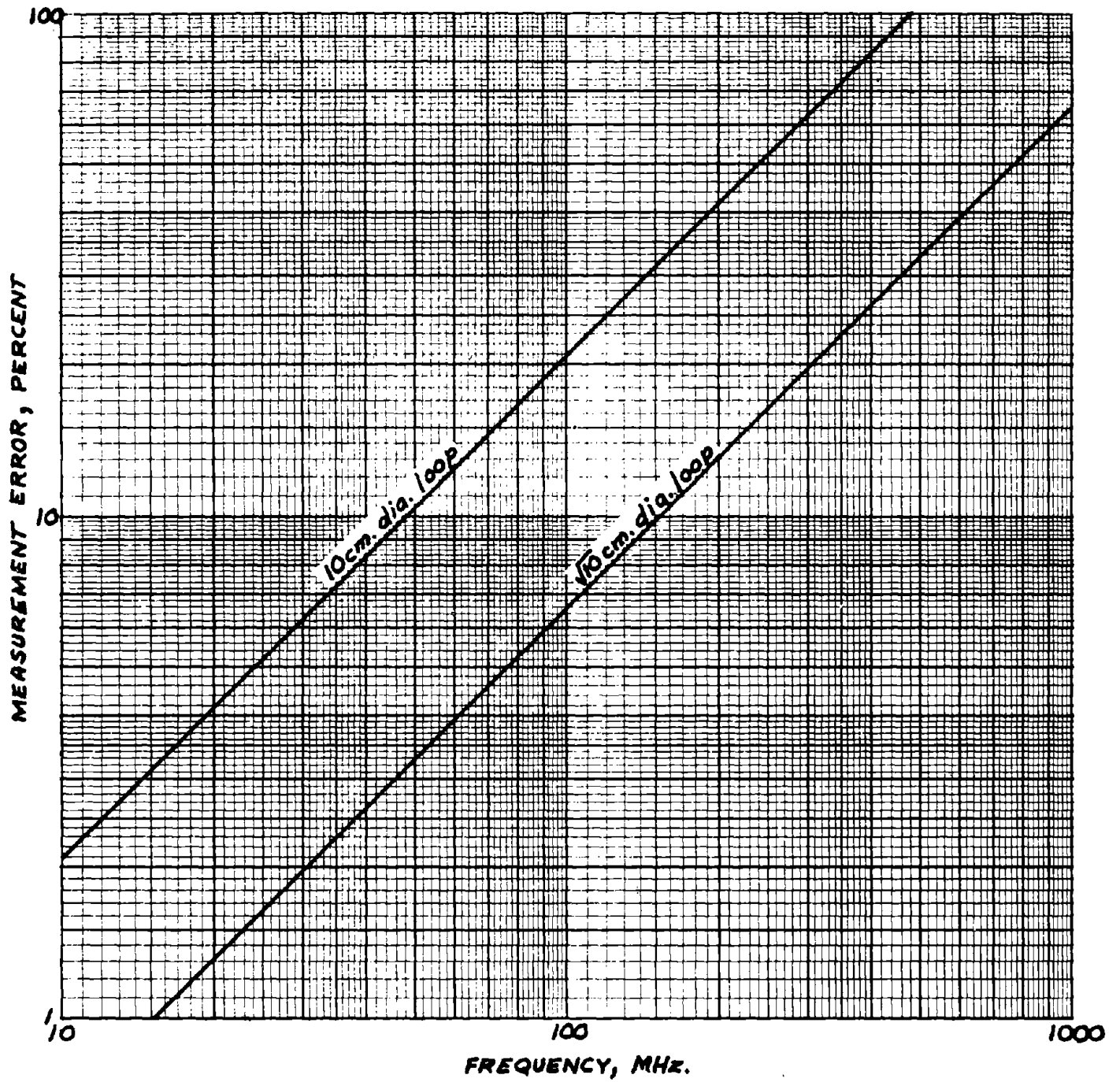


Figure 6. Worst-Case Measurement Error of the 10-cm and the 3.16-cm diameter Loop Antennas due to their Electric-Dipole Response.

### 3. Partial-Resonance Effect in a Loop Antenna

Partial resonance is the result of the combined effect of the distributed capacitance of the loop and the gap and diode capacitances, represented by  $C_a$  in figure 2.

Using the simplified circuit diagram shown in figure 7, the response can be written<sup>5</sup>

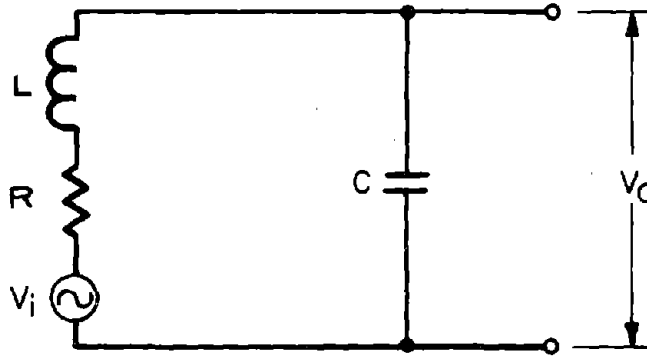


Figure 7. A Simplified Equivalent Circuit of the Loop Probe.

$$\frac{V_o}{V_i} = \frac{-j \frac{1}{\omega C}}{R + j\left(\omega L - \frac{1}{\omega C}\right)} = \frac{-j \frac{\omega_o}{\omega}}{\frac{1}{Q} + j\left(\frac{\omega}{\omega_o} - \frac{\omega_o}{\omega}\right)}, \quad (14)$$

where  $Q = \frac{X_o}{R}$ ,  $X_o = 2\pi f_o L = \frac{1}{2\pi f_o C}$ ,  $\omega_o = 2\pi f_o$ , and  $f_o$  is the self-resonant frequency of the loop. The resistance,  $R$ , is assumed to remain constant with frequency, but turns out to be negligible anyway, as will be seen.

The magnitude of equation (14) can be rearranged to give

$$\left| \frac{V_o}{V_i} \right| = \frac{1}{1 - \delta^2} \left[ 1 + \frac{\delta^2}{Q^2(1 - \delta^2)^2} \right]^{-\frac{1}{2}}, \quad (15)$$

<sup>5</sup>Terman, F.E., Electronic and Radio Engineering, pp. 44-57 (McGraw-Hill Book Co., Inc., New York, N.Y., 1955).

where  $\delta = \omega/\omega_0$  is the ratio of the operating frequency to the resonant frequency of the loop. It can be shown that if  $Q > 10$ , and  $\delta < 0.75$ , the second term within the bracket will be negligible, and equation (15) will simplify to

$$\left| \frac{V_o}{V_i} \right| \approx \frac{1}{1 - \delta^2}. \quad (16)$$

Equation (16) can be used to estimate the required correction in the loop measurement for values of  $\delta$  up to 0.75, and is shown plotted in figure 8. The correction is also shown plotted vs. frequency for the 10 cm and 3.16 cm diameter loop in figure 9. Under the above conditions these corrections are essentially independent of the  $Q$  of the loop (that is, independent of its losses) and depends only on the ratio,  $\omega/\omega_0$ , defined above. The approximate self-resonant frequencies for the two loop probes are given in Table II.

Table II

Approximate Self-Resonant Frequencies of the Loop Probes

<u>Loop Diameter</u>	<u>Frequency</u>
10.00 cm	280 MHz
3.16 cm	760 MHz

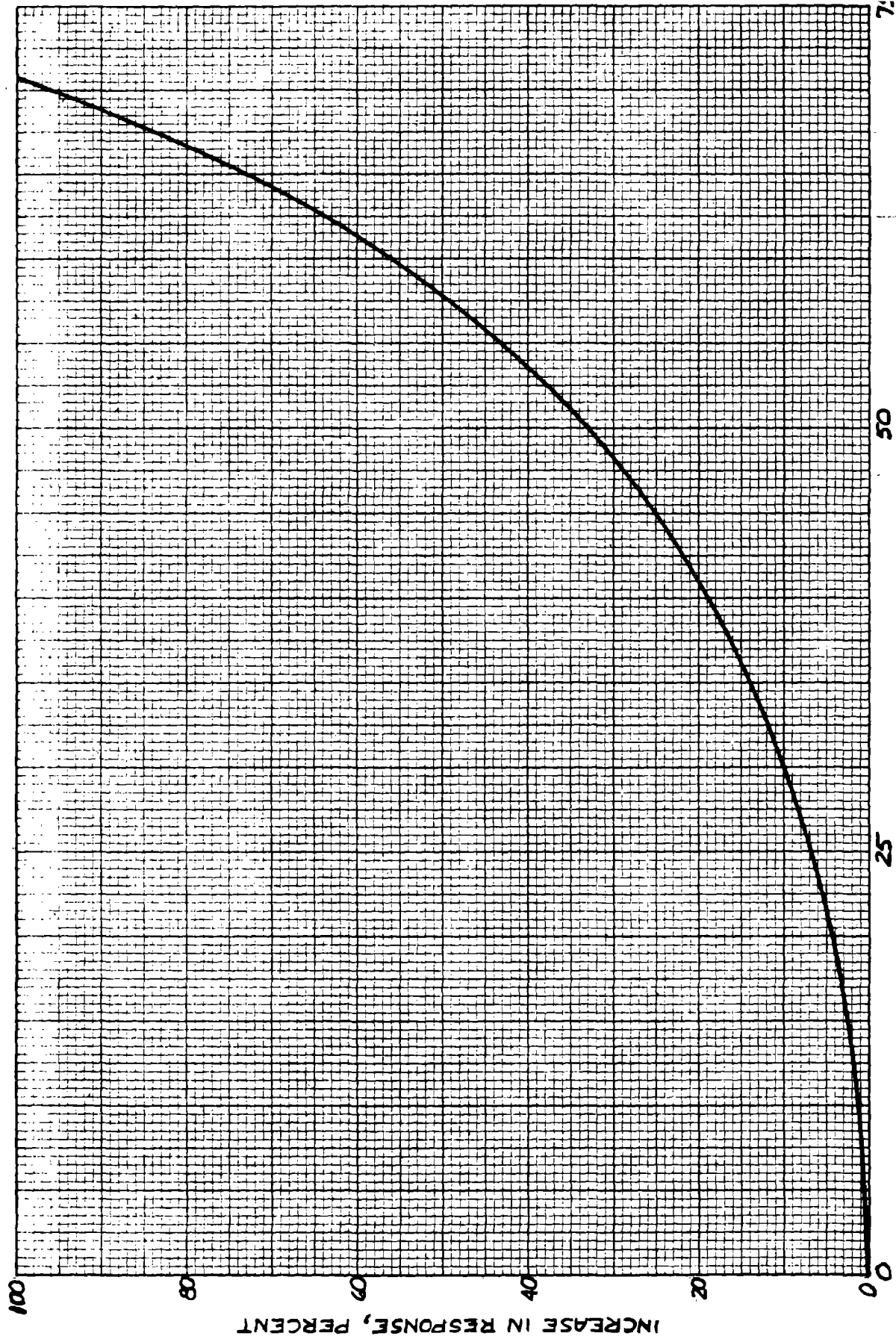


**Figure 8.** Increase in the Response of a Loop Antenna due to Partial Resonance.

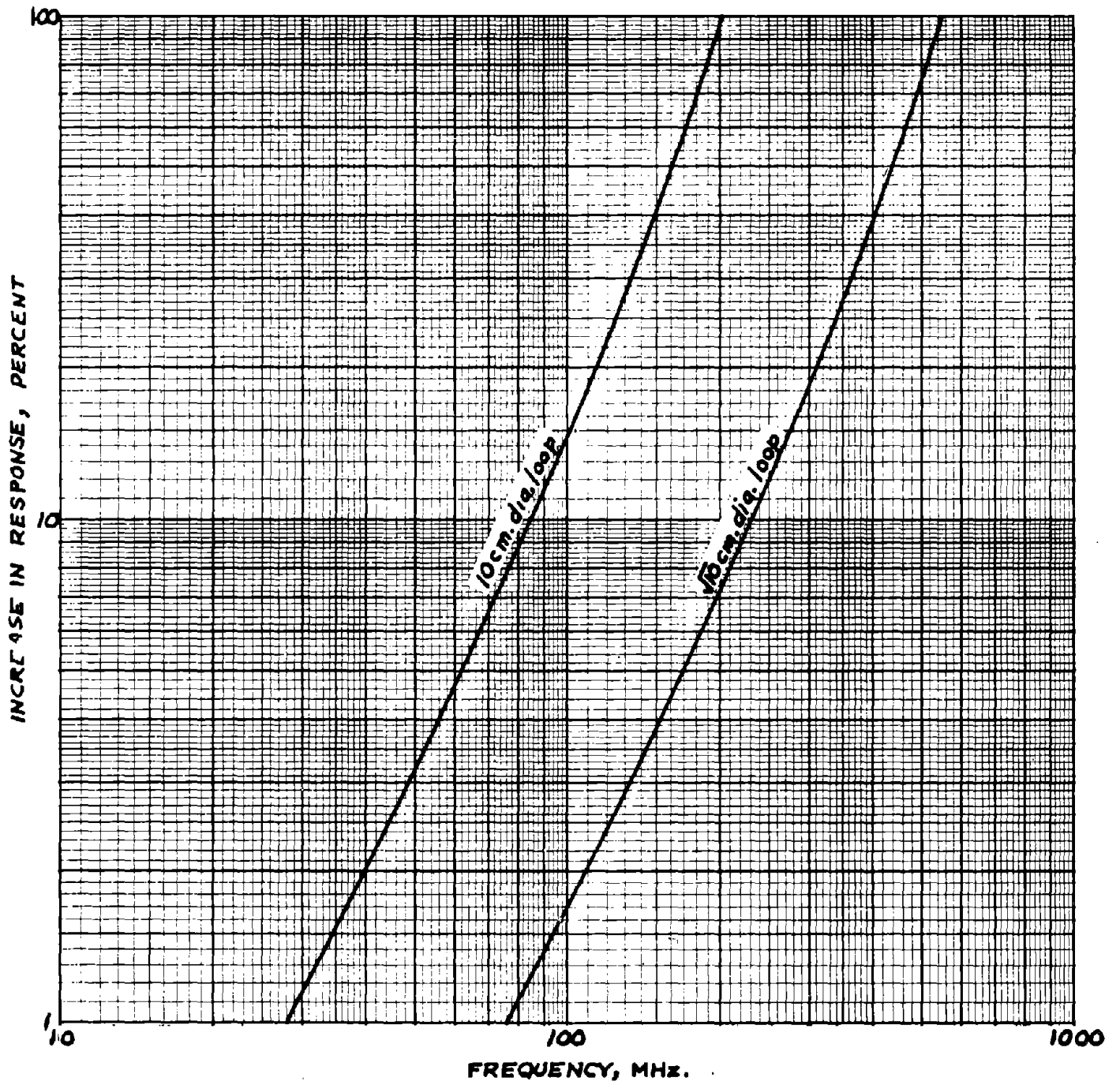


Figure 9. Increase in the Response of the 10-cm and the 3.16-cm Diameter Loop Antennas due to Partial Resonance.

#### 4. The NBS Conducting-Plastic Transmission Line

4.1 Introduction. In the past, it has been found difficult to accurately measure the absolute strength of electromagnetic fields having a complex spatial distribution over a significant range of magnitudes. Part of the difficulty has been in the use of a metallic r-f transmission line between the dipole measuring antenna and the receiver, or selective voltmeter, located at a point remote from the antenna. Such metallic lines often cause large measurement errors because the line not only perturbs the field being measured, but the unwanted r-f currents induced on the line contribute to the total response of the field-strength meter.

One method of avoiding this difficulty is to use some form of radio, optical, or acoustical telemetering transmitter in place of the metallic line. This transmitter, located at the measuring antenna, can be used to transmit the desired information to a remote readout unit. This technique has been employed in various ways by a number of experimenters in the field. However, because of the nature and complexity of the telemetering instrumentation, the resulting devices have had varying degrees of success, but in general have been seriously limited in the usable range of frequencies and magnitudes over which absolute measurements could actually be made.

The NBS near-zone field-strength meters being described in this report avoid these telemetering difficulties by making use of a special technique. The complex telemetering instrumentation, mentioned above, is eliminated by transmitting the detected output of the measuring antenna over a completely non-metallic electrical transmission line which does not appreciably interact with the field being measured. If the transmission line is made of sufficiently high-resistance material, it will be essentially "transparent" to the surrounding field. Thus, it will not interact appreciably with the field being measured or have unwanted coupling with the measuring antenna. This is to say that the r-f currents induced in the transmission-line by the field will be negligibly small, resulting in insignificant reradiation, or that any r-f energy propagating along the line will be heavily attenuated because of the extremely high loss of the line. However, the detected d-c output voltage of the measuring antenna can be transmitted without appreciable loss if a high-resistance d-c vacuum-tube voltmeter or electrometer is used as the readout device at the receiving end of the line.

4.2 Conducting-Plastic Materials. The high-resistance, non-metallic transmission lines used by NBS employ conducting-plastic monofilaments in place of the usual copper conductors. In the type of material used, the plastic matrix is made conducting to the desired extent by filling (up to 30 percent) with finely powdered carbon (carbon black) during initial stages of manufacture while the plastic is in a more or less liquid or molten form. The finely divided carbon is dispersed throughout the plastic to make as homogeneous a mixture as possible. Electrical conduction results from actual physical contact between the carbon particles suspended in the plastic matrix. Not all plastics lend themselves to this application. Only certain types of plastic molecules will properly accept carbon particles in a manner which renders the material electrically conducting, without a deleterious effect on the final mechanical properties. For example, nylon is one of the types which, so far, has been found to be unsuitable by various manufacturers. Several types of conducting-plastic were tested at NBS for this purpose. The most suitable was found to be conducting-Teflon made to NBS specifications.

4.3 Construction of the Conducting-Teflon Transmission Line. The parallel-conductor balanced transmission line was constructed using two 0.03 inch diameter nylon-coated, conducting-Teflon monofilaments, each approximately 30 feet in length. Each filament was in turn pulled through a separate 1/8 inch diameter, vinyl-coated, woven-fiber-glass sleeve for added strength and insulation. These two 30-foot lengths were then pulled together through an equal length of heat-shrinkable irradiated-polyvinyl chloride tubing, which served as the outer jacket of the parallel-conductor line. Conducting silver cement was used to electrically bond the ends of the conducting-Teflon filaments to the special twin-connector plugs at both ends of the line. The oversized outer vinyl jacket was then shrunk in place over the entire length of line, and over the plugs at the ends, as well, so as to make them an integral part of the line. A high-temperature heat gun was used to perform the shrinking.

The completed 30-foot length of line was tested in a high-level electromagnetic field. The interaction with the field was found to be approximately two orders of magnitude less than that found for the copper line used as a reference. A high noise level was found to exist on the line, due to changing contact resistance between the carbon particles (when the line was flexed). This noise was found to average approximately 0.2 volt on open circuit, and approximately 0.02 volt when one end of the line was terminated in

a resistance of 10 megohms. However, since the d-c level transmitted over this line was in the range from 1 to 10 volts, the "flexural" noise did not present a problem. The Teflon line was found to be considerably more stable electrically than the other plastic lines tested, and therefore was adopted for use with NBS near-zone field-strength meters.

#### 4.4 Electrical Characteristics of the Conducting-Teflon Line.

Conductor Resistance. The nominal volume resistivity of the conducting-Teflon plastic material used is 3 ohm-cm. The measured d-c resistance of this material in 0.03-inch-diameter-monofilament form is 20,000 ohms per lineal foot, giving a loop resistance for the twin-conductor balanced line of 40,000 ohms per foot.

Mutual Capacitance. The mutual capacitance between the parallel conductors of this line, as measured at a low audio frequency, is approximately 10 picofarads per foot.

Propagation Function. The degree of interaction of the conducting plastic transmission line with the field being measured is directly related to the line loss, or attenuation, of the resulting wave induced on the line. By making the attenuation sufficiently great, this interaction can be reduced to negligible proportions. The propagation function of this transmission line can be derived from the classical transmission line equations to be found in any engineering text on the subject.<sup>6</sup> This theory becomes only approximate in the case of the lossy line, however, and is offered here only to illustrate the degree of attenuation to be expected for such a line. In regard to the electrical parameters of this line, it can be shown, at least for frequencies below 100 MHz, that the series inductive reactance per unit length,  $\omega L$ , is negligible compared to the series resistance per unit length,  $R$ , and that the shunt conductance per unit length,  $G$ , is negligible compared to the shunt susceptance per unit length,  $\omega C$ . That is  $\omega L \ll R$ , and  $G \ll \omega C$ . When these conditions are substituted in the complete equations for the attenuation and phase functions of the reflectionless transmission line, the following expressions are obtained:

$$\text{Attenuation Function } \alpha \cong \left[ \frac{\omega CR}{2} \right]^{1/2}, \text{ nepers per unit length. (17)}$$

$$\text{Phase Function } \beta \cong \left[ \frac{\omega CR}{2} \right]^{1/2}, \text{ radians per unit length. (18)}$$

<sup>6</sup>Ramo, S., Whinnery, J.R., and VanDuzer, T., Fields and Waves in Communication Electronics, pp. 45-51 (John Wiley & Sons, Inc., New York, N.Y., 1965).

It is interesting to note that for this case, both the attenuation and phase functions are given by the same expression. These quantities both increase as the square root of frequency over the frequency range for which the equations are valid.

4.5 Transmission Line Attenuation. The attenuation per unit length along the line can be determined approximately from equation (17) for both the balanced- and the common-modes of propagation, by substituting in appropriate values of  $R$  and  $C$ . The use of the values  $R = 40,000$  ohms/foot, and  $C = 10$  pF/foot, given previously, yields a balanced-mode attenuation of approximately 6.1 nepers (53 dB) per foot at a frequency of 30 MHz for the conducting-Teflon line. To determine the common-mode attenuation, the two transmission-line conductors are considered as operating in parallel, making  $R' = 10,000$  ohms/foot. The value of resistance to use in equation (17) is  $R = 2R' = 20,000$  ohms/foot. If the insulated line is lying flat on the ground plane, its capacitance,  $C'$ , to the plane can be considered to be approximately four times that given previously, or 40 pF/foot (assuming the spacing between conductors to be double their height above the image plane). The value of capacitance to use in equation (17) is then  $C = C'/2 = 20$  pF/foot. This, then, results in the same  $R$ - $C$  product, and therefore the same attenuation for the common-mode case as for the balanced-mode of propagation.

Thus, it can be seen that the line loss at 30 MHz for either mode of propagation is extremely high for the conditions assumed. This means that the r-f current flowing at any point along the portion of transmission line, lying on the ground plane, will be attenuated by more than 40 dB (100X) in traveling a distance of only one foot. The common-mode attenuation decreases somewhat for the short portion of line near the probe, since its capacitance to the plane is less. However, this has presented no observable difficulty, as long as this section of line is maintained normal to the probe axis to preserve the electrical symmetry. From actual tests made on this line in an electromagnetic field, the attenuation achieved in this line appears to be sufficient to reduce the interaction with the field to negligible proportions.

The attenuation was measured in the laboratory from d-c to 100 MHz using a conducting-Teflon monofilament as the center conductor of a 5-foot length of rigid coaxial line having a copper outer conductor 1.25 inches inside diameter. The measured attenuation agreed with the theoretical, based on classical transmission-line theory, to within a proportion of 1 dB in 10 over the above frequency range. The results are shown plotted in figure 10.

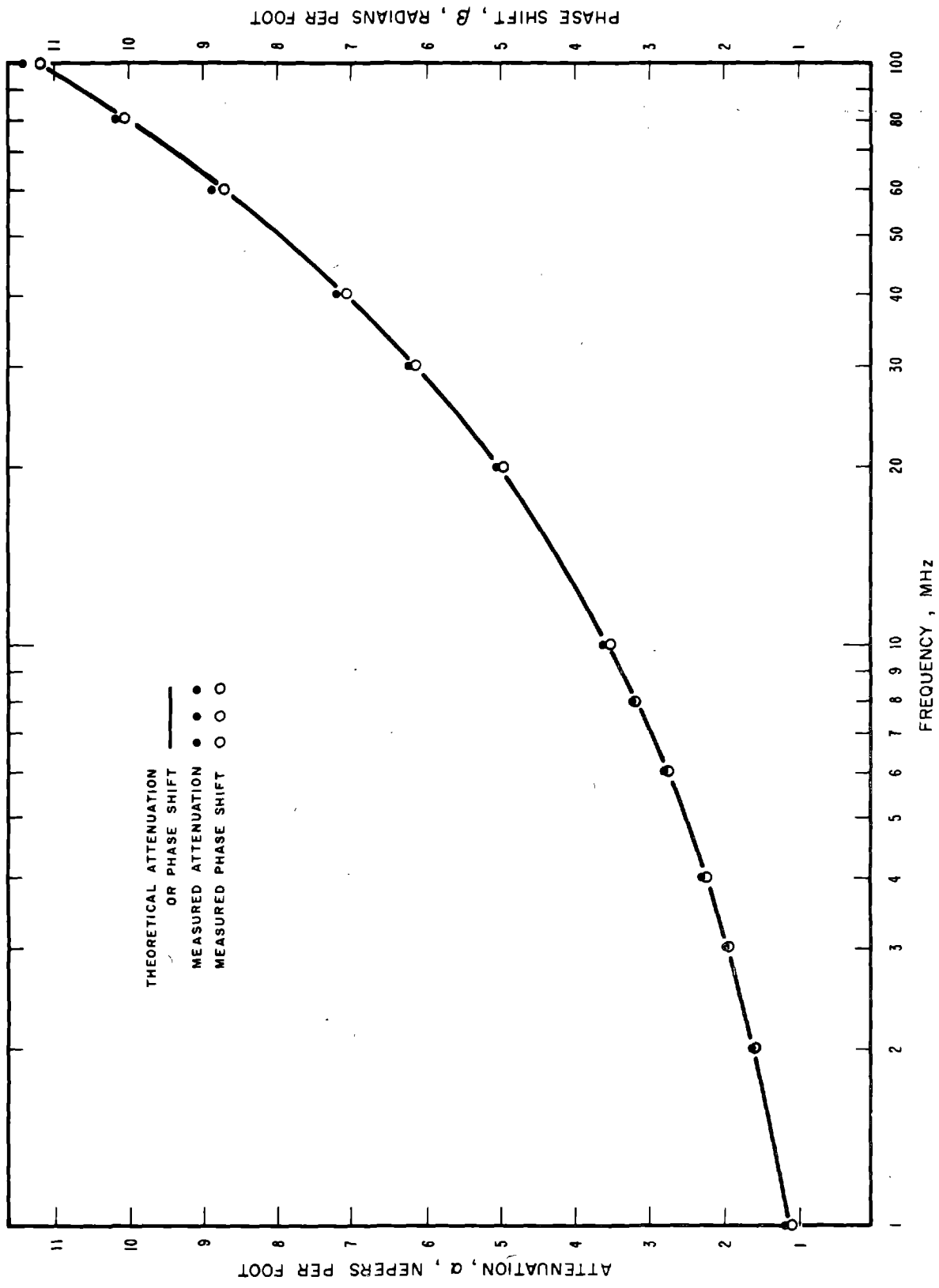


Figure 10. Attenuation and Phase-Shift of the Conducting-Plastic Transmission Line.

As can be seen from equations (17) and (18), the phase shift, in radians, along the line is equal to the attenuation in nepers for the same distance. It is a little surprising to find that the 30-foot line used in our tests is one-half wavelength long at approximately 10 kHz, due to the extremely rapid phase shift along the line. Conversely, the velocity of propagation,  $v$ , along the line is extremely low, as can be determined from equation (19), which is based on the relation,  $v = \omega/\beta$ .

$$v \cong \left[ \frac{2\omega}{CR} \right]^{1/2}, \text{ unit distance per second.} \quad (19)$$

The velocity of propagation for the above line is approximately  $0.094 v_0$ , at a frequency of 30 MHz, where  $v_0$  = free-space velocity. The velocity is proportional to  $(\omega)^{1/2}$  over the frequency range for which equation (19) is valid.<sup>7</sup>

---

<sup>7</sup>Greene, F.M., A New Near-Zone Electric-Field-Strength Meter, NBS J. of Res., 71-C, No. 1, pp. 51-57 (Jan.-Mar. 1967).

## 5. Summary and Conclusions

The development and construction of two portable, magnetic-field strength probes by the Electromagnetics Division of the National Bureau of Standards for the National Institute for Occupational Safety and Health are described in this report. These probes are intended for use in measuring hazard-level magnetic near fields in the frequency range from approximately 10 to 40 MHz. They will be used by the NIOSH in their EM radiation-exposure program for determining the biological effects of hazard-level, non-ionizing EM fields on human beings.

These probes consist of small, single-turn, balanced loop antennas 10-cm and 3.16-cm in diameter. Their measuring range varies with frequency but averages from roughly 0.5 to 5.0 and from 5.0 to 50 amperes per meter, respectively, over the above frequency range.

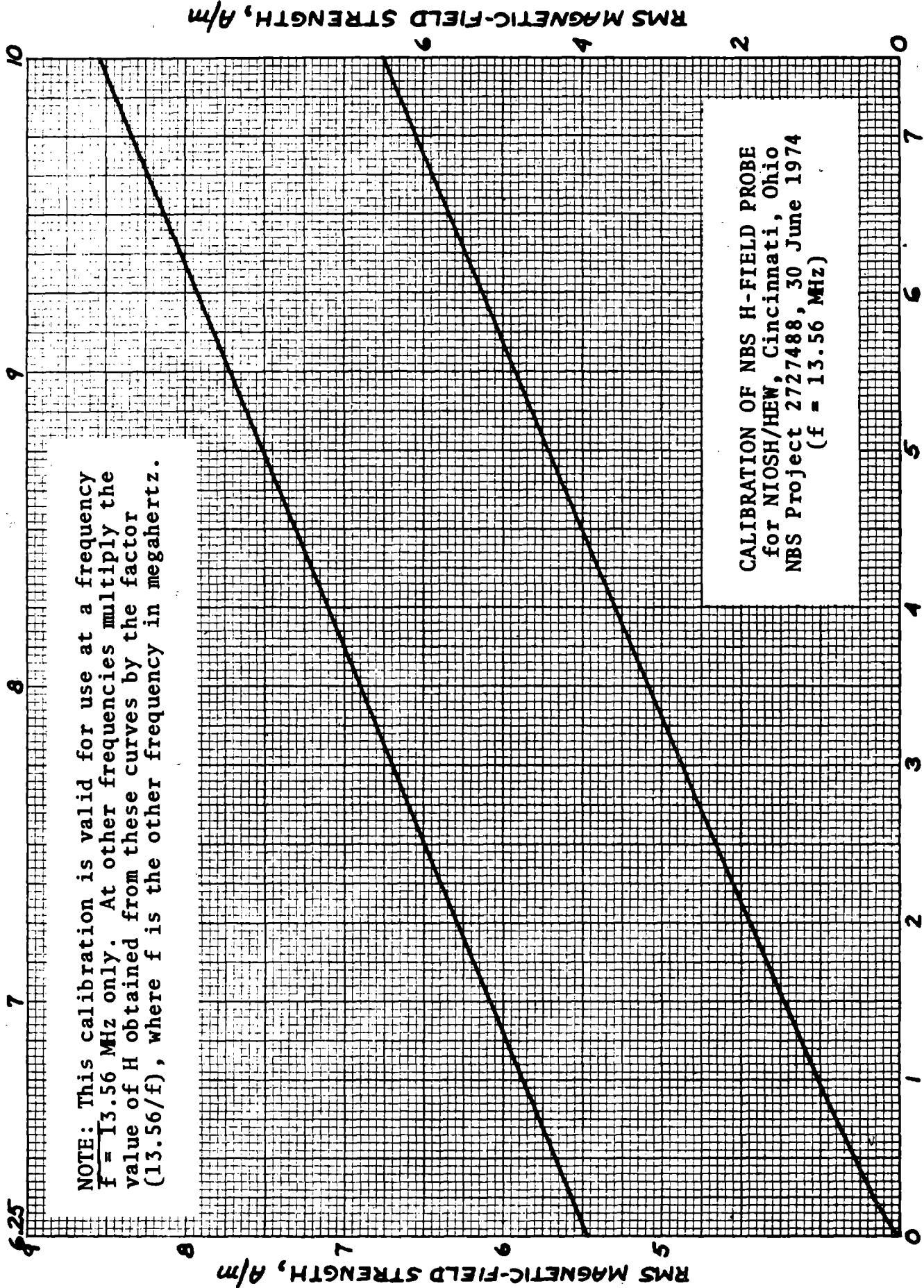
The response of the loop probes as a function of their operating frequency and physical size has also been analyzed in this report. In addition measurement errors were evaluated resulting from: (a) the electric-dipole response of the loops to the electric field present; (b) partial resonance within the loops due to their distributed capacitance; and (c) harmonic frequencies present in the fields being measured. The characteristics of the high-resistance, conducting-plastic transmission line, developed at NBS, were also discussed in detail in Section 4.

The worst-case errors resulting from the electric-dipole response are proportional to frequency for a fixed-size of loop. At a frequency of 40 MHz this error is 8.3 percent for the 10-cm diameter loop and 2.6 percent for the 3.16-cm diameter loop as can be determined from equation (13) or figure 6. These errors can be essentially eliminated by following the experimental procedure outlined near the end of Section 2.

The errors due to partial resonance are roughly proportional to the square of the frequency as can be determined from equation (16) or figure 9. At a frequency of 40 MHz this error is only 2 percent for the 10-cm diameter loop and 0.5 percent for the 3.16-cm diameter loop and can usually be considered negligible.

Careful attention should be paid to errors resulting from harmonic fields present in the field being measured. As an example, consider a third harmonic field that is 30 dB below the fundamental-frequency field being measured. This harmonic is roughly 3 percent of the fundamental in magnitude. The basic response of a loop is proportional to frequency as shown by equation (4) or figure 3. Therefore, the magnitude of the harmonic will be enhanced by a factor of three from 3 percent to 9 percent from this cause. The electric-dipole response and partial resonance of the loop will further increase this to a worst-case error due to this one harmonic of 14 percent for the 10-cm loop and 10 percent for the 3.16-cm loop as can be determined from figures 6 and 9. If the effect of only one additional harmonic were taken into account, these worst-case errors could easily be doubled. This, of course, would be in addition to the other errors discussed. There is no simple way of accurately evaluating these harmonic errors unless the actual harmonic content of the field is known.

PROBE DC OUTPUT VOLTS



RMS MAGNETIC-FIELD STRENGTH, A/m

RMS MAGNETIC-FIELD STRENGTH, A/m

PROBE DC-OUTPUT VOLTS

PROBE DC-OUTPUT VOLTS

7

8

9

10

NOTE: This calibration is valid for use at a frequency  $f = 27.12$  MHz only. At other frequencies multiply the value of H obtained from these curves by the factor  $(27.12/f)$ , where f is the other frequency in megahertz.

RMS MAGNETIC-FIELD STRENGTH, A/m

4

3

2

1

0

RMS MAGNETIC-FIELD STRENGTH, A/m

3

2

1

0

CALIBRATION OF NBS H-FIELD PROBE  
for NIOSH/HEW, Cincinnati, Ohio  
NBS Project 2727488, 30 June 1974  
( $f = 27.12$  MHz)

PROBE DC-OUTPUT VOLTS

0

1

2

3

4

5

6

7

8

9

10

PROBE DC-OUTPUT VOLTS

PROBE DC-OUTPUT VOLTS

